15th EAWE PhD Seminar on Wind Energy
29–31 October 2019
Centrale Nantes, France

Calibration of onshore wind turbine numerical model using experimental data

F Pimenta[a], C M Branco[b], C M Teixeira[c], and F Magalhães[a]

[a]CONSTRUCT - ViBest, Faculty of Engineering of the University of Porto
[b]Faculty of Engineering of the University of Porto
[c]VESTAS Porto Design Center

E-mail: ec09176@fe.up.pt

Abstract

A numerical model was created with FAST developed by the National Renewable Energy Laboratory (NREL).The structural and mechanical properties of the structure were calculated from the geometric properties of the tower and blades. The aerodynamic properties of different sections of the blades were computed with a 2D model created with ANSYS Fluent. Having the wind turbine fully characterised, the control mechanisms were calibrated from the manufacturer catalogues.

Numerous time series of wind excitation for different operation conditions were generated, and the structural response computed. In paralell the Supervisory Control and Data Acquisition (SCADA) operating in parallel with a series of extensometers and accelerometers located in strategic points along a real wind turbine tower and blades provided a full description of the internal forces in both locations and the estimation of the modal properties for different operating conditions.

Both measured and simulated response allowed the identification and validation of structural dynamic properties and static and dynamic internal loads. The results obtained from the numerical model were in good agreement with the ones measured in the field. This preliminary validation is important to extrapolate the model to more demanding scenarios, as the ones experienced by floating wind turbines where due to the lack of experimental data available for floating wind turbines the procedures being used in other structures need to be tested with numerically simulated data.

Keywords:Wind Turbine Modelling, Operational Modal Analysis, CFD, FAST

1 Introduction

The main objective of this work is to set the way to a reliable off-shore wind turbine numerical model which can then be used to simulate the structure response and test alternative monitoring strategies algorithms for data processing. In a first approach it is fundamental to develop a model that can adequately reproduce the behaviour of onshore wind turbines, which results can be validated with experimental data. For that purpose a wind turbine located in Tocha, Portugal monitored in the context of the WindFarmSHM project with the experimental monitoring system described in detail in [1] was chosen as case study. This paper describes how the numerical model was obtained as well as the different validations made by comparing numerical with experimental results.

2 Numerical Model

The modelled wind turbine is a 100 [m] rotor diameter and 93.3 [m] tower height VESTAS V100 with 1.8MW rated power capable of working between 4 [m/s] and 20 [m/s]. The accuracy of the results obtained is strongly dependent of both structural properties and loads acting on the structure. While the first point can be obtained without great difficulty the former is mainly influenced by the aerodynamic properties of the blades. To accurately model both effects it was used FAST software and a brief description of the software main principles is needed.

2.1 Structural Properties

The static and dynamic response of the structure to any loads that are to be applied are mainly dependent of the behaviour of the tower and blades. As FAST uses a generalized degree of freedom approach based on the modal configuration of the tower, a finite element model was made to obtain this configurations.

In this initial FEM model the tower was simulated providing the linear mass density and SS/FA stiffness in 37 points distributed along its height. The blades were discretized in 49 different sections and to each section were associated 2 directions stiffness, density and structural twist. As only the external geometry of the blades and its global mass were known the stiffness properties and variation of linear weight were scaled from the 5MW baseline turbine available in FAST certification tests [2]. The chord scale (k_C) was calculated as the ratio between the chord of the VESTAS V100 and the reference blade. Assuming these can be treated as thin wall hollow sections then the mass scale can be obtained directly from the product of the chord and thickness scale (k_t). Matching the global mass obtained for both allowed to calculate the latter. With this assumption, the inertia scale (k_I) for each section can finally be calculated as the product of the 3^{rd} power of the chord scale by the global thickness scale. The foundation was modelled with shell elements with properties taken from execution project drawings.

The two principal modes configuration for the tower in each direction were deducted from the tangent line at the tower base so that they respect FAST assumption of 0 slope at in this section and fitted to a 6^{th} degree polynomial with unitary displacement on the top of the tower as required [3].

In the FAST model the foundation was assumed to have infinite stiffness to translations and rotation about the tower yaw axis and the remaining component of the stiffness matrix were evaluated from the bending moment and rotation of tower base of the FEM model described. To simulate this effect, it was used the HydroDyn module with an imposed linear stiffness matrix only.

2.2 Aerodynamic Properties

The aerodynamic properties of the blades are an input of FAST and can be calculated with carefully built CFD models. The CFD model properties used to obtain the lift and drag forces (F_L and F_D respectively) and corresponding coefficients for the different angles of attack (α) for the adopted airfoils were previously validated with the well-documented NACA0012 airfoil which was object of wind tunnel experiments [4]. In order to capture the variation of the aerodynamic properties along the blade, it was divided in 10 different sections equally spaced - Figure 1 - and a CFD model was made for each, for different angles of attack. The adopted conventions are defined in Figure 2.

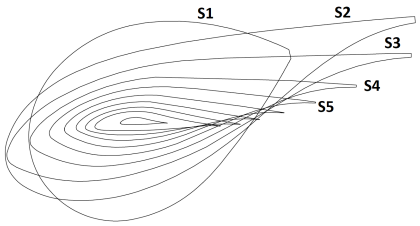

Figure 1: Representation of the adopted blade sections.

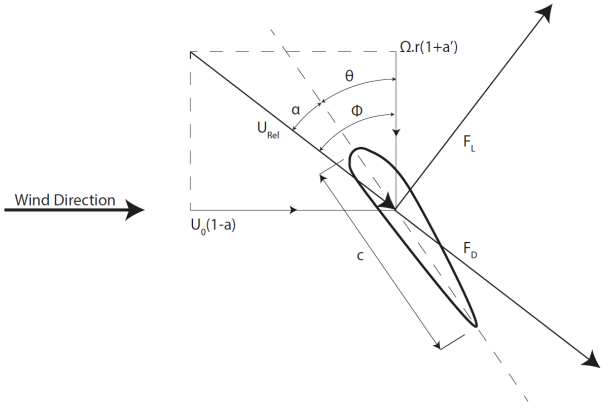

Figure 2: Representation of the adopted forces conventions for a given wind (U_0) and rotor speed (Ω) [5].

2.2.1 CFD model validation

The CFD simulation was carried out with ANSYS/fluent code based on the Reynolds Average Navier Stokes Equations (RANS). As described in [6] the Spalart-Allmaras (SA) turbulence model [7] has been sistematically tested over the years and provided accurate results at least for the precision assumed

necessary in this work. It was also used the SST k-ω turbulence model as it captures both the accurate formulation of standard k-ω model in the near-wall region and freestream independence of the k-ϵ model in the far field [8] . The airfoil was treated as a no-slip wall and all the equations were solve using second order schemes only. The pressure and velocity plots of the airfoil at 0^o angle of attack are presented in Figure 3 as well as the mesh used.

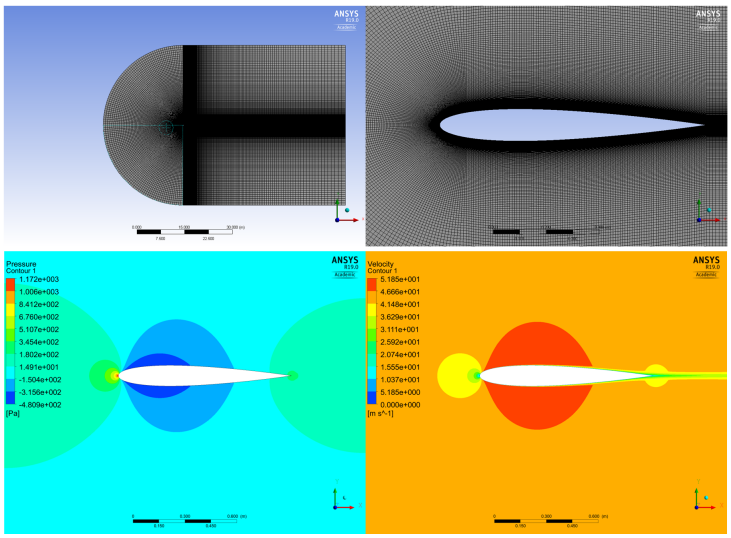

Figure 3: Mesh used in the CFD simulation (on top) and pressure (on the bottom left) and velocity (on the bottom right) plots for 0^o angle of attack on NACA0012 airfoil.

The lift and drag forces were computed for several angles of attack with both turbulence models in a 1 [m] chord NACA 0012 airfoil and 43.82 [m/s] wind speed, which guarantees close Reynolds and Mach numbers similarity with the experimental results obtained by Ladson in [9]. Figure 4 represents these coefficients for all the angles of attack tested.

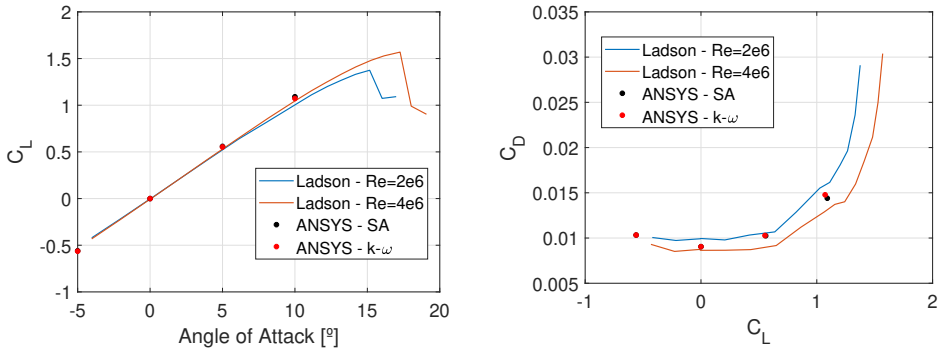

Figure 4: Lift and drag coefficients validation.

Both models are in good agreement with the experimental results used for comparison and while the lift coefficient before stall is mainly Reynols number independent the same does not apply to the drag coefficient where higher Reynolds number lead to lower drag forces.

2.2.2 CFD results

As the simulations for angles of attack (AoA) higher that stall angle become more complex it is important to understand the values that the different sections will experiment during the wind turbine operation

conditions. This evaluation can be made using Blade Element Theory (BEM) expressions - equations 1 and 2.

$$U_{rel} = \sqrt{U_0^2 \times (1-a)^2 + \Omega^2 \times r^2 \times (1+a')^2} \tag{1}$$

$$\tan\phi = \tan(\alpha+\theta) = \frac{U_0 \times (1-a)}{\Omega \times r \times (1+a')} \tag{2}$$

However, as the forces decomposition depend on the axial and tangential induction coefficients (a and a' respectively) that by turn depend on the forces, an iterative process is needed. Defining the blade solidity (σ_r) as the ratio between the blades area and the rotor area it is possible to write an expression for both induction coefficients based on the parameters of the previous iteration - equations 3 and 4, where $C_{\parallel}$ and $C_{\perp}$ represent the component of the lift and drag forces in and out of the rotor plane respectively.

$$\frac{a}{1-a} = \frac{\sigma_r}{4 \cdot sen^2(\phi)} \cdot \left[C_{\parallel}(a) - \frac{\sigma_r}{4 \cdot sen^2(\phi)} \cdot C_{\perp}^2(a) \right] \tag{3}$$

$$\frac{a}{1+a'} = \frac{\sigma_r \cdot C_{\perp}(a)}{4 \cdot sen(\phi) \cdot cos(\phi)} \tag{4}$$

In order to evaluate the angles of attack that will be necessary for each blade, it was assumed a linear behaviour near the 0º angle of attack so that the lift coefficient could be computed based on equation 5 with slope (m) and zero lift angle of attack (α_0) obtained from CFD simulations between -5º and 5º. It was also assumed the expression for the drag coefficient obtained for a fully laminar boundary layer over a flat plate so that its value depends on the Reynolds number only and can be calculated from equation 6 [10].

$$C_L = m \times (\alpha - \alpha_0) \tag{5}$$

$$C_D = \frac{1.328}{Re} \tag{6}$$

Knowing the structural twist distribution and chosing the pitch angle in accordance to the SCADA system records, it is possible to obtain the angles of attack for the 9 last sections presented in Figure 5[1]. The expected angles of attack are within a rather short range which can be analysed with the CFD model. All sections were tested for AoA between -10º and 12º and Reynols number equal to 2×10^6, which was chosen as a representative value for the different operating conditions.

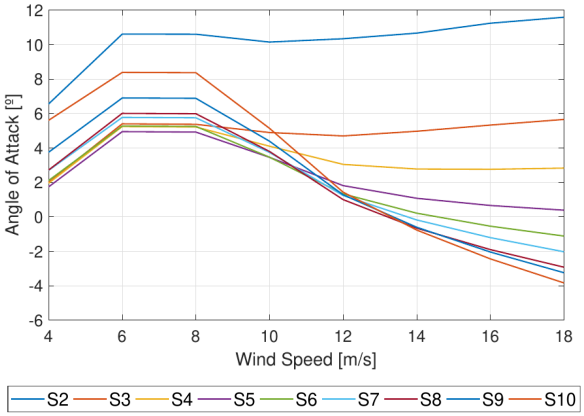

Figure 5: Angles of attack expected for the different airfoils as a function of wind speed.

Having the drag and lift coefficients for this angles of attack two important corrections should be considered. The first one is to correct the values to take into account the 3D stall delay caused by a

[1]The first section is not analysed as it was considered a circular section with constant lift and drag coefficients.

rotating blade. This can be achieved by the methods proposed by Selig in 1998 [11] and Eggers in 2003 [12] for the lift and drag coefficients respectively. Furthermore, as only angles of attack in a restricted domain were tested and a full description for any other value maybe needed during a simulation, it is important to extrapolate the values at larger angles of attack. This was made using the Viterna extrapolation method [13]. The representation of lift and drag coefficients for one of the airfoils can be seen in Figure 6.

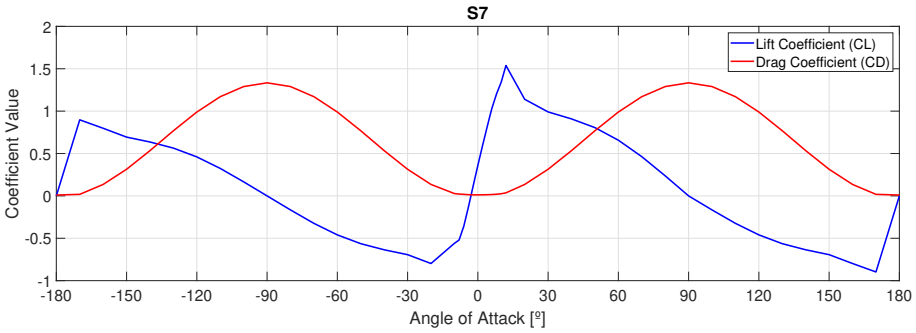

Figure 6: Lift and Drag coefficients for the full range of AoA obtained for section S7.

2.3 Control Systems Simulation

The control system properties were defined using the simplified routines presented in [14]. As there was no available information about the pitch angles below rated speed, it was necessary to look into the SCADA data and define an average minimum pitch angle that was fed into the pitch control routine beside the rated rotor speed.

The torque control was defined so that the power output would match the theorethical values, setting the appropriate values of gear box efficieny, power law coefficient of Region 2 and Rated Torque value of Region 3[2]. As Region 2 is assumed to have constant pitch angle and constant speed, an infinite number of equilibrium values between aerodynamic torque and resistant torque can be defined associated with different rotor speed and hence different thrust forces due to different angles of attack. Having this in mind, the power law coefficient was defined by an iterative process in order to minimize the differences between theorethical and numerical thrust forces. The gear box efficiency can then be calibrated matching the theoretical power output with the generator speed obtained in the last iteration of the previous step. The rated torque value can be defined from the already determined gear box efficiency and rated speed so that the theoretical rated power is achieved for wind speed above 12 [m/s]. The power and thrust curves obtained from the simulations at steady states for different wind speeds can be seen in Figure 7.

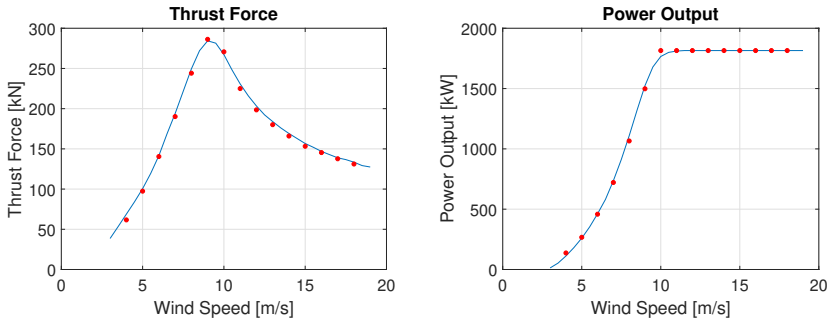

Figure 7: Comparison between simulated values (red points) and theorethical data (blue line).

[2]The mentioned regions are in accordance with the nomenclature used in [14]. Region's 2 torque is assumed to be proportional to the 2^{nd} power of generator speed and Region's 3 torque is assumed to be constant.

3 Results

With the model fully characterised, it is now possible to compare the numerical and experimental data available. In order to validate the simulated response a comparison of some characteristic curves can be made with the SCADA data and further validations can be obtained comparing the internal forces and dynamic properties derived from simulated and measured datasets.

3.1 Natural frequencies

The natural frequencis of the structure were obtained applying operation modal operation analysis techniques to the accelerations provided by the numerical model. The response of the structure was simulated during 30 minutes with the rotor stopped and then divided in shorter series of 300 [s]. The power spectrum was calculated for each separately and then averaged. The spectrum from the acceleration simulated at 75% of the tower height can be compared with the ones measured in the same conditions. While the 1^{st} mode can be accurately predicted the 2^{nd} mode presents bigger deviations from experimental data. As this mode strongly depends on the interaction between tower and blades it was needed to calibrate both blades stiffness through an additional global scale factor and the spring used to simulate the drivetrain flexibility. The spectrum obtained from both experimental and simulated data (after and before correction) can be seen in Figure 8, where it is marked a reference value for the ressonant frequencies obtained from experimental data.

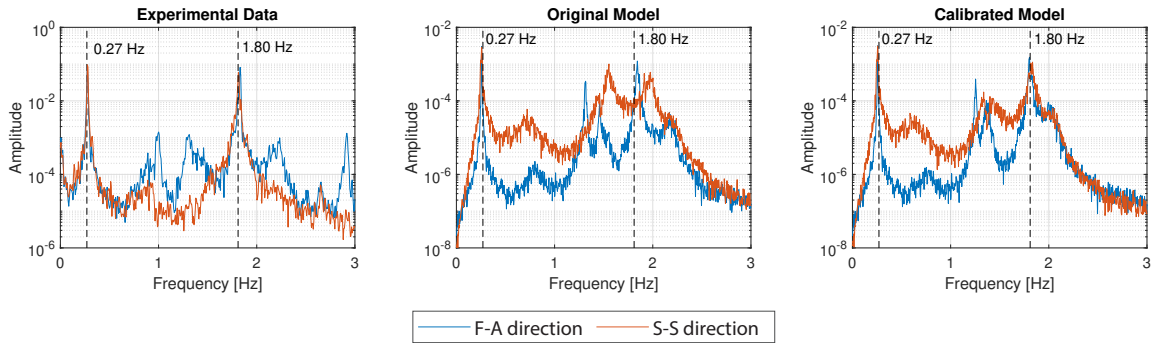

Figure 8: Power spectrum estimation for a stopped rotor experimental and numerical results before and after calibration.

After the calibration, the principal ressonant frequencies are correctly identified but other peaks of smaller amplitude are not correctly obtained. Based on the experimental data and the FE model, these frequencies are associated with mode shapes mainly dependent on the blades behaviour. This results can be explained by all the simplifcations made in the structural and mechanical properties of the blades.

3.2 SCADA curves

After model calibration, the first test can be made comparing the numerical power, rotor speed and pitch curves with the ones recorded by the SCADA system - Figure 9. Analyzing the rotor speed and pitch angle curve it is clear that the control implemented reproduced adequately the values obtained from SCADA system for wind speeds above 5 [m/s]. The results associated with lower wind speeds are not a major concern, as they are associated with low forces. The power output seems to be in good agreement with the expected value for all the tested scenarios.

3.3 Bending Moments

In order to compare the internal forces of the model with the ones measured, a selection of some 10 minutes interval with wind speed oscillating around an approximately constant mean value was used. To select such intervals, the SCADA data from February was analysed and 10-minute time intervals with the properties presented in Table 1 were selected.

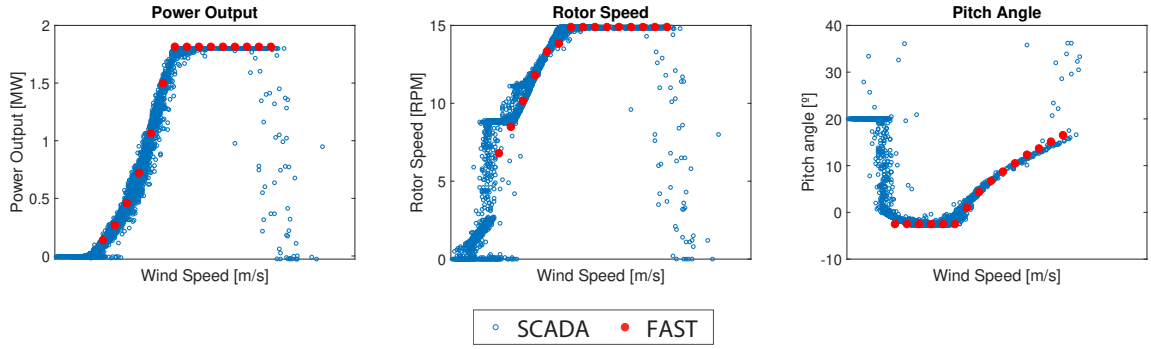

Figure 9: Comparison between numerical and experimental curves.

Table 1: 10-minute time intervals selected for validation of the FAST model

Date	**Mean Wind Speed [m/s]**	**Turbulence Intensity [%]**	**Yaw Angle [º]**
01/02/2019 21:20	13.90	22.30	325.2
01/02/2019 21:40	13.70	8.76	317.0
10/02/2019 15:20	5.70	19.30	357.4

Based on these wind characteristics it was possible to construct 3 dimensional wind grids with equivalent mean speed and turbulence intensity with TurbSim preprocessor from NREL [15]. For this series it was assumed a power law mean wind profile with shear coefficient of 0.20 and surface roughness of 0.03 [m]. The time series of bending moments on the tower section instrumented with strain gauges (6.5 [m] above tower base) of both experimental and numerical data can be seen in Figure 10.

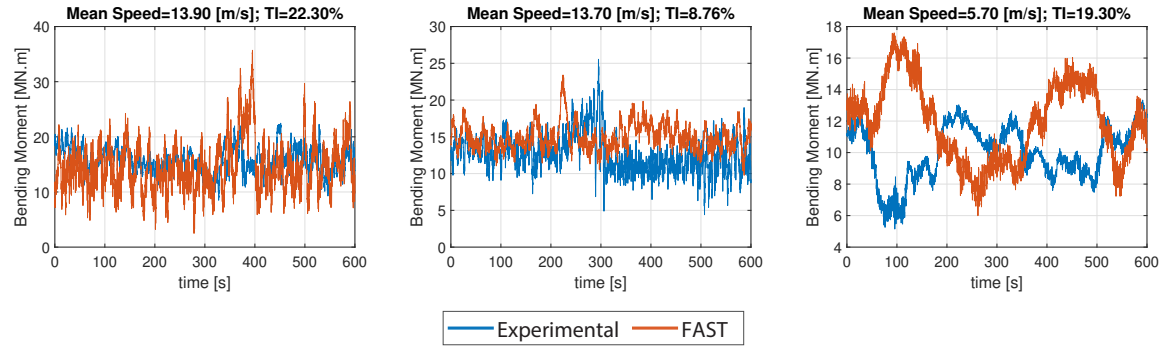

Figure 10: Comparison between numerical and experimental curves.

Although numerical and experimental statistical properties comparison is only possible with a large number of simulations, a visual comparison of the series offers a first evaluation of the quality of the results that are in good agreement with the experimental ones.

4 Conclusions

The developed model was able to make suitable predictions of the thrust force and power output using only data from project drawings and theoretical curves. To obtain good results regarding the dynamic behaviour of the structure it was fundamental the calibration with the experimental data, which allowed to correctly identify the principal global modes of the structure. The frequency peaks associated with blades local modes were not identified correctly but the global response is in good agreement even with

the simplifiactions and assumptions that were needed. In future works it is important to define the blades with more correct information and extend the validations made to local internal forces and modal response of the blades.

Acknowledgements

The support of EDP Renewables and VESTAS in greatly acknowledged. This work was also financially supported by: PhD Grant SFRH/BD/138980/2018, UID/ECI/04708/2019- CONSTRUCT - Instituto de I&D em Estruturas e Construções and the project PTDC/ECI-EST/29558/2017, both funded by national funds through the FCT/MCTES (PIDDAC).

References

[1] Pacheco J, Magalhães F and Magalhães S 2019 *15^{th} EAWE PhD Seminar*

[2] Jonkman J, Butterfield S, Musial W and Scott G 2009 Definition of a 5-MW reference wind turbine for offshore system development Tech. Rep. NREL/TP-500-38060 National Renewable Energy Lab

[3] Jonkman J M, Buhl Jr M L *et al.* 2005 Fast user's guide Tech. Rep. NREL/EL-500-38230

[4] McCroskey W J 1987 A critical assessment of wind tunnel results for the NACA 0012 airfoil Tech. Rep. NASA-A-87321 National Aeronautics and Space Administration Ames Research Center

[5] Burton T, Sharpe D, Jenkins N and Bossanyi E 2001 *Wind Energy Handbook* (John Wiley and Sons)

[6] 2D NACA 0012 airfoil validation case *https : //turbmodels.larc.nasa.gov/naca*0012*_val.html* accessed: 2019-09-09

[7] Spalart P and Allmaras S 1992 *American Institute of Aeronautics and Astronautics* **439**

[8] Menter F 1993 *American Institute of Aeronautics and Astronautics* **93-2906**

[9] Ladson C L 988 Effects of independent variation of Mach and Reynolds numbers on the low-speed aerodynamic characteristics of the NACA 0012 airfoil section Tech. Rep. NASA-TM-4074, L-16472, NAS 1.15:4074 National Aeronautics and Space Administration Ames Research Center

[10] Anderson J D 2001 *Fundamentals of Aerodynamics* Aeronautical and Aerospace Engineering Series (McGraw-Hill)

[11] Du Z and Selig M 1998 *ASME 1998 Wind Energy Symposium* vol 20 (American Society of Mechanical Engineers Digital Collection) pp 9–19

[12] Eggers A J, Chaney K and Digumarthi R 2009 *ASME 2003 Wind Energy Symposium* (American Society of Mechanical Engineers Digital Collection) pp 283–292

[13] Viterna L A and Janetzke D C 1982 Theoretical and experimental power from large horizontal-axis wind turbines Tech. rep. National Aeronautics and Space Administration, Cleveland, OH (USA)

[14] Malcolm D and Hansen A 2002 Windpact turbine rotor design study: June 2000-June 2002 (Revised) Tech. Rep. NREL/SR-500-32495 National Renewable Energy Laboratory

[15] Jonkman B J and Buhl Jr M L 2006 Turbsim user's guide Tech. rep. National Renewable Energy Lab